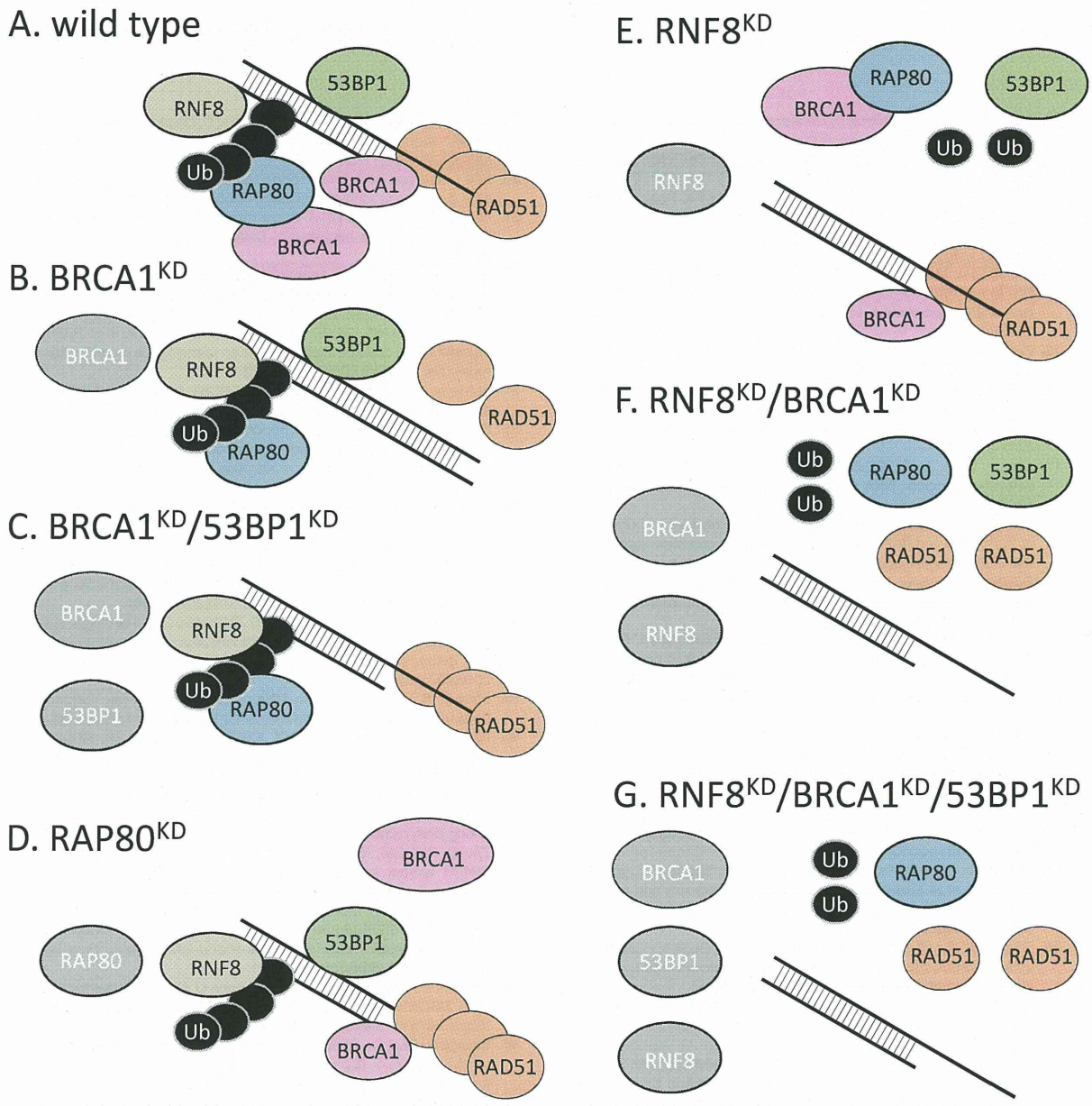


**Supplementary Figure 1. A schematic of the assembly of DNA damage response-related proteins at DSB sites. A**, Ubiquitin chain, RAP80, BRCA1, 53BP1 and RAD51 assemble at DSB sites in normal cells. **B,** The ubiquitin chain, RAP80 and 53BP1 but not RAD51 assemble at DSB sites in BRCA1-depleted cells. **C,** The ubiquitin chain, RAP80 and RAD51 assemble at DSB sites in BRCA1/53BP1-depleted cells. **D,** The ubiquitin chain, a small subset of BRCA1 protein, 53BP1 and RAD51 assemble at DSB sites in RAP80-depleted cells. **E,** A small subset of BRCA1 protein and RAD51 but not the ubiquitin chain or 53BP1 assemble at DSB sites in RNF8-depleted cells. **F, G,** The ubiquitin chain, RAD51, BRCA1 and 53BP1 do not assemble at DSB sites in RNF8/BRCA1-depleted cells or RNF8/BRCA1 /53BP1-depleted cells.

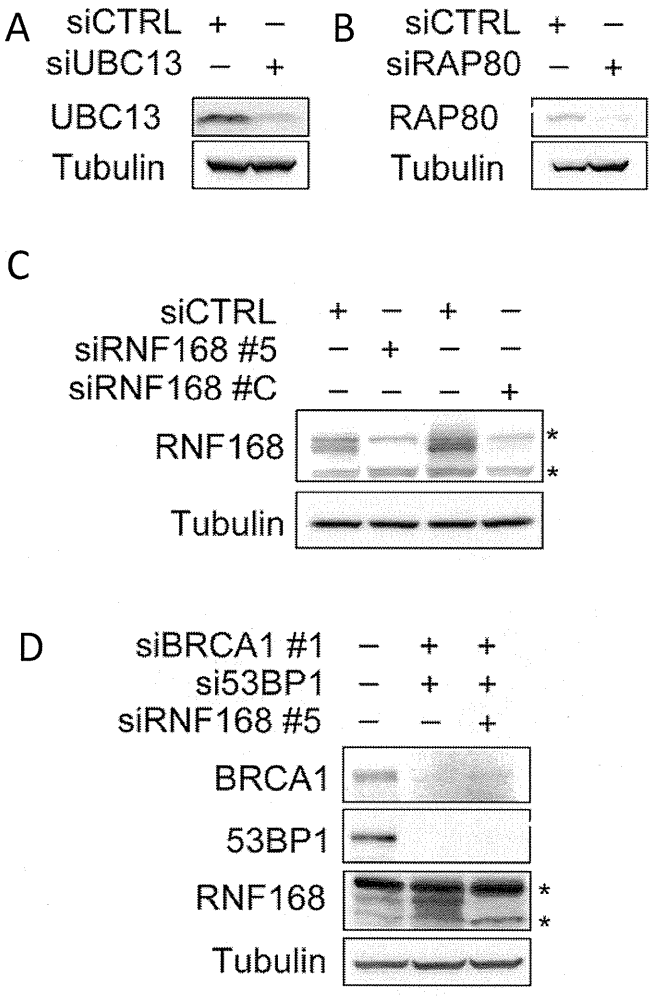


**Supplementary Figure 2. The effective knockdown of UBC13, RAP80 or RNF168 was confirmed using western blotting.** U2OS **(A)**, HeLa **(B)** or HCT116 **(C, D)** cells transfected with indicated siRNAs were subjected to western blotting for the indicated proteins. *non-specific bands.

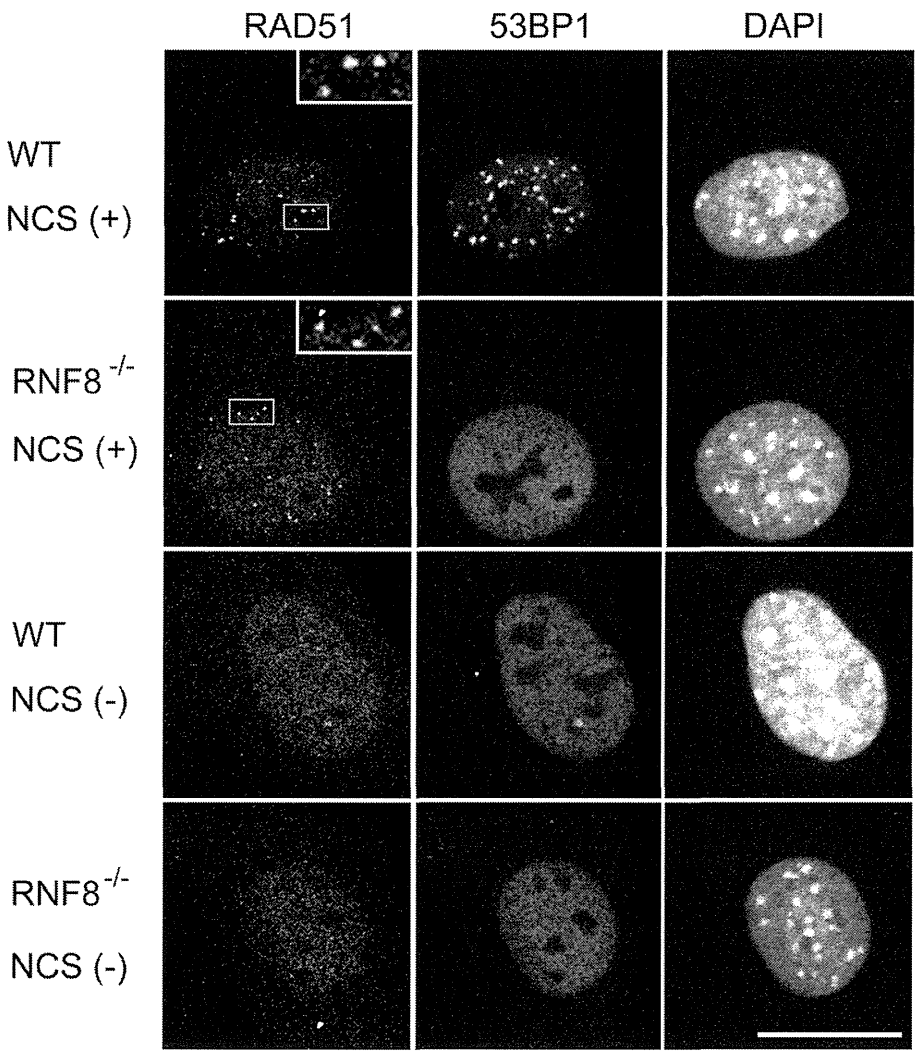


**Supplementary Figure 3. RAD51 assembles at DSB sites in RNF8$^{-/-}$ MEFs.** WT and RNF8$^{-/-}$ MEFs were treated with 5 ng/ml NCS for 10 min and then subjected to immunofluorescence with the indicated antibodies at 5 hr post-NCS treatment. The area enclosed by each rectangle is magnified. Scale bar, 10 μm

A

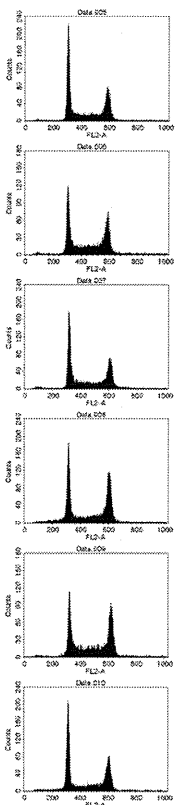

siCTRL
S-G2 phase: 47.4%

siBRCA1 #1
S-G2 phase: 56.0%

siRNF8 #D
S-G2 phase: 51.0%

siRNF8 #2
S-G2 phase: 54.7%

siBRCA1 #1 + siRNF8 #D
S-G2 phase: 60.2%

siBRCA1 #1 + siRNF8 #2
S-G2 phase: 47.9%

B

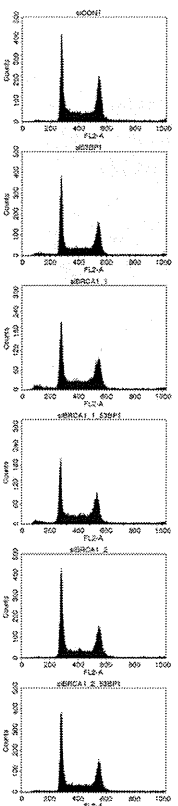

siCTRL
S-G2 phase: 54.2%

si53BP1
S-G2 phase: 47.8%

siBRCA1 #1
S-G2 phase: 50.0%

siBRCA1 #1 + si53BP1
S-G2 phase: 50.6%

siBRCA1 #2
S-G2 phase: 47.4%

siBRCA1 #2 + si53BP1
S-G2 phase: 49.5%

C

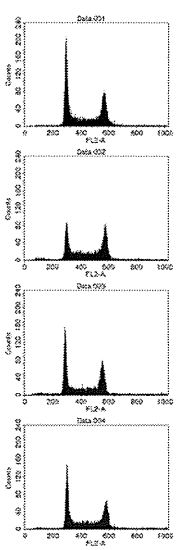

siCTRL
S-G2 phase: 49.3%

siRNF8 #D + siBRCA1 #1 + si53BP1
S-G2 phase: 61.8%

siRNF8 #2 + siBRCA1 #1 + si53BP1
S-G2 phase: 53.3%

siBRCA1#1 + si53BP1
S-G2 phase: 51.5%

**Supplementary Figure 4. Cell cycle analysis.** HCT116 cells transfected with various combinations of non-targeting, BRCA1-specific, 53BP1-specific and RNF8-specific siRNAs were fixed, stained with PI and then subjected to cell-cycle analysis using flow cytometry. BRCA1 and RNF8 were simultaneously depleted **(A)**. BRCA1 and 53BP1 were simultaneously depleted **(B)**. RNF8, BRCA1 and 53BP1 were simultaneously depleted **(C)**.

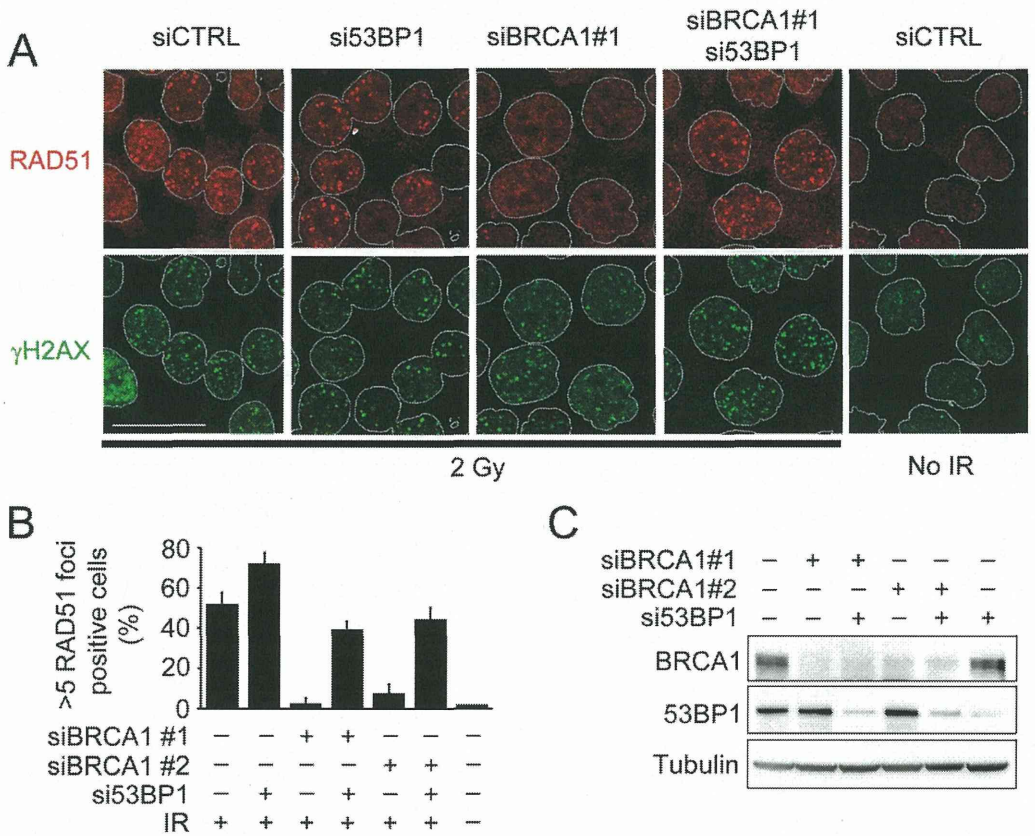


**Supplementary Figure 5. Depletion of 53BP1 rescues RAD51 assembly at DSB sites in BRCA1-depleted human cells. A-B**, HCT116 cells transfected with the indicated siRNAs were irradiated with 2 Gy and analyzed for RAD51 and gH2AX immunofluorescence at 6 h post-ionizing radiation. Representative images. Scale bar, 25 μm **(A)**. The quantification of cells with >5 RAD51 foci (mean ± s.d., *N* = 3) **(B)**. **C**, HCT116 cells transfected with the indicated siRNAs were subjected to western blotting for the indicated proteins.

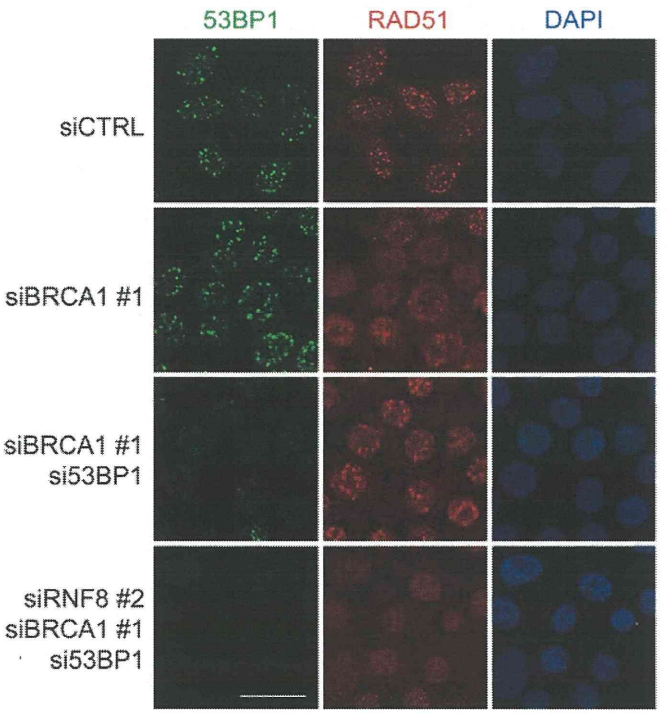


**Supplementary Figure 6. RNF8 suppresses RAD51 assembly in BRCA1/53BP1-depleted 293T cells.** 293T cells transfected with the indicated siRNAs were irradiated with 2 Gy and analyzed for RAD51 and 53BP1 immunofluorescence at 4 h post-ionizing radiation. Representative images. Scale bar, 25 μm

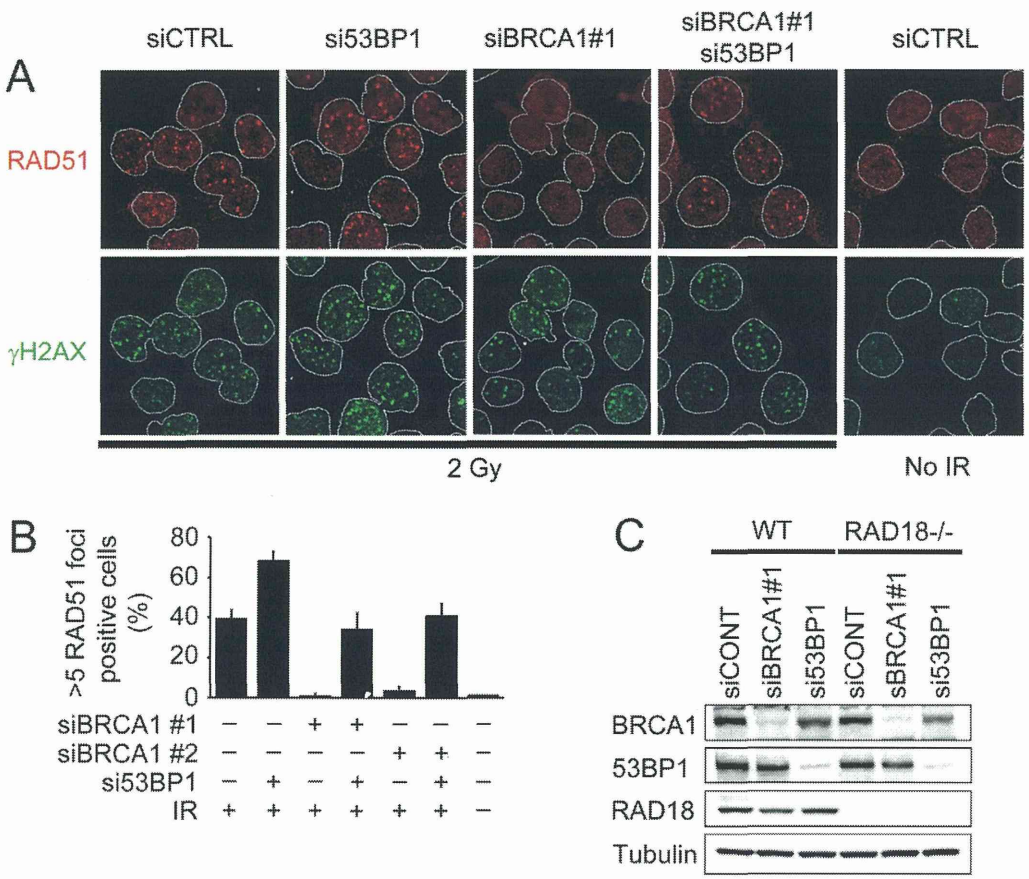


**Supplementary Figure 7. RAD18 is not required for RAD51 assembly at DSB sites in the absence of BRCA1 and 53BP1. A-B**, *RAD18*$^{-/-}$ HCT116 cells transfected with the indicated siRNAs were irradiated with 2 Gy and analyzed for RAD51 and gH2AX immunofluorescence at 6 h post-ionizing radiation. Representative images. Scale bar, 25 μm **(A)**. The quantification of cells with >5 RAD51 foci (mean ± s.d., *N* = 3) **(B)**. **C**. HCT116 (WT) and *RAD18*$^{-/-}$ HCT116 cells transfected with indicated siRNAs were subjected to western blotting for the indicated proteins. The expression level of BRCA1 and 53BP1 was similar in and *RAD18*$^{-/-}$ HCT116 cells

HORM CANC (2013) 4:1–11
DOI 10.1007/s12672-012-0126-6

ORIGINAL PAPER

# Intratumoral Estrogen Concentration and Expression of Estrogen-Induced Genes in Male Breast Carcinoma: Comparison with Female Breast Carcinoma

**Kiyoshi Takagi · Takuya Moriya · Masafumi Kurosumi · Kimako Oka · Yasuhiro Miki · Akiko Ebata · Takashi Toshima · Shoji Tsunekawa · Hiroyuki Takei · Hisashi Hirakawa · Takanori Ishida · Shin-ichi Hayashi · Junichi Kurebayashi · Hironobu Sasano · Takashi Suzuki**

Received: 10 August 2012 / Accepted: 8 October 2012 / Published online: 18 October 2012


**Abstract** It is speculated that estrogens play important roles in the male breast carcinoma (MBC) as well as the female breast carcinoma (FBC). However, estrogen concentrations or molecular features of estrogen actions have not been reported in MBC, and biological significance of estrogens remains largely unclear in MBC. Therefore, we examined intratumoral estrogen concentrations, estrogen receptor (ER) α/ERβ status, and expression profiles of estrogen-induced genes in MBC tissues, and compared these with FBC. 17β-Estradiol concentration in MBC ($n$=4) was significantly (14-fold) higher than that in non-neoplastic male breast ($n$=3) and tended to be higher than that in FBC ($n$=7). Results of microarray analysis clearly demonstrated that expression profiles of the two gene lists, which were previously reported as estrogen-induced genes in MCF-7 breast carcinoma cell line, were markedly different between MBC and FBC. In the immunohistochemistry, MBC tissues were frequently positive for aromatase (63 %) and 17β-hydroxysteroid dehydrogenase type 1 (67 %), but not for steroid sulfatase (6.7 %). A great majority (77 %) of MBC showed positive for both ERα and ERβ, and its frequency was significantly higher than FBC cases. These results suggest that estradiol is locally produced in MBC

K. Takagi (✉) · T. Suzuki
Department of Pathology and Histotechnology,
Tohoku University Graduate School of Medicine,
2-1 Seiryo-machi, Aoba-ku,
Sendai, Miyagi-ken 980-8575, Japan
e-mail: k-takagi@med.tohoku.ac.jp

T. Moriya
Department of Pathology 2, Kawasaki Medical School,
Kurashiki, Japan

M. Kurosumi
Department of Pathology, Saitama Cancer Center,
Saitama, Japan

K. Oka · H. Hirakawa
Department of Surgery, Tohoku Kosai Hospital,
Sendai, Japan

Y. Miki · H. Sasano
Department of Anatomic Pathology,
Tohoku University Graduate School of Medicine,
Sendai, Japan

A. Ebata · T. Ishida
Department of Surgical Oncology,
Tohoku University Graduate School of Medicine,
Sendai, Japan

T. Toshima
Department of Surgery, Tohoku Rosai Hospital,
Sendai, Japan

S. Tsunekawa
Department of Surgery, Kansai Electric Power Hospital,
Osaka, Japan

H. Takei
Division of Breast Surgery, Saitama Cancer Center,
Saitama, Japan

S.-i. Hayashi
Department of Molecular and Functional Dynamics,
Tohoku University Graduate School of Medicine,
Sendai, Japan

J. Kurebayashi
Department of Breast and Thyroid Surgery,
Kawasaki Medical School,
Kurashiki, Japan

H. Sasano
Department of Pathology, Tohoku University Hospital,
Sendai, Japan

tissue by aromatase. Different expression profiles of the estrogen-induced genes may associate with different estrogen functions in MBC from FBC, which may be partly due to their ERα/ERβ status.

## Introduction

Male breast carcinoma (MBC) is an uncommon disease, and its incidence is less than 1 % of that in female breast carcinoma (FBC). However, it has been increasing in recent years [1]. Because of the low incidence, MBC has not been studied well, and limited information is available regarding the epidemiology, pathogenesis, and treatment [2]. Therefore, it is very important to examine the biological features of MBC in order to improve clinical outcome of the patients.

It is well known that estrogens contribute immensely to the development and/or progression of FBC. Concentration of biologically active estrogen estradiol is significantly high in FBC tissues, and it is locally produced from circulating inactive steroids by estrogen-producing enzymes, such as aromatase (conversion from circulating androstenedione to estrone or testosterone to estradiol), steroid sulfatase (STS; hydrolysis of circulating estrone sulfate to estrone), and 17β-hydroxysteroid dehydrogenase type 1 (17βHSD1; conversion of estrone to estradiol) [3]. Estrogen actions are initiated by binding of estrogens with estrogen receptors (i.e., ERα or ERβ), followed by transactivation of the target genes. Various estrogen-responsive genes have been identified in the breast carcinoma [4, 5], and analyses of these genes have greatly contributed to better understanding of molecular functions of estrogen actions in FBC [6]. The estrogen actions are considered to be mainly mediated through ERα in FBC [7, 8], and endocrine therapies, such as anti-estrogens (tamoxifen, etc.), aromatase inhibitors, and gonadotropin-releasing hormone (GnRH) agonists, are used in patients with ERα-positive FBC patients.

Estrogens are also speculated to play important roles in MBC, and tamoxifen is used in MBC patients as an endocrine therapy [9]. Various studies have demonstrated frequent expression of ERα in MBC tissues as well as ERβ and progesterone receptor (PR) [10–12], and immunolocalization of aromatase has been also reported in MBC [13]. However, intratumoral concentration of estrogens or expression of other estrogen-producing enzymes has not been reported in MBC. Moreover, no information is available regarding the expression profiles of estrogen-responsive genes in MBC, to the best of our knowledge. Therefore, it remains unclear whether estrogen actions and/or effectiveness of endocrine therapy in MBC could be the same as that in FBC.

Therefore, in this study, we examined intratumoral concentrations of estrogens, immunolocalization of estrogen-producing enzymes, and expression profiles of estrogen-induced genes in MBC tissues, and compared these findings with those in FBC, in order to examine the significance of estrogens in MBC.

## Materials and Methods

### Patients and Tissues

Two sets of tissue specimens were used in this study. The first set is composed of 14 snap-frozen specimens. Among these, four MBC tissues were obtained from patients who underwent surgical treatment from 2009 to 2010 at Tohoku University Hospital (Sendai, Japan), Tohoku Kosai Hospital (Sendai, Japan), Tohoku Rosai Hospital (Sendai, Japan), and Kansai Electric Power Hospital (Osaka, Japan). The mean age of these patients was 65 years (range, 62–67). Three non-neoplastic breast tissues were also collected from patients who underwent surgical treatment at Tohoku University Hospital, Tohoku Kosai Hospital, and Saitama Cancer center (Saitama, Japan; mean age, 65 years; range, 62–67 years), which were not matched with the carcinoma specimens. As a control group, seven specimens of FBC were obtained from postmenopausal patients who underwent surgical treatment from 2001 to 2003 at Tohoku University Hospital (mean age, 57 years; range, 50–69 years). These specimens were stored at −80 °C for subsequent hormone assays. Eight specimens of MBC and FBC were also used in microarray analysis.

The second set is composed of 102 specimens of breast carcinomas fixed in 10 % formalin and embedded in paraffin wax. Among these, 30 MBC tissues were obtained from patients who underwent surgical treatment from 1975 to 2010 at Tohoku University Hospital, Tohoku Kosai Hospital, Tohoku Rosai Hospital, Saitama Cancer Center, Sendai, and Kawasaki Medical School Hospital (Okayama, Japan). As a control group, we also used 72 FBC tissues collected from postmenopausal women who underwent surgical treatment from 1984 to 1992 at Tohoku University Hospital.

Research protocol was approved by Ethics Committee at Tohoku University School of Medicine.

### Liquid Chromatography/Electrospray Tandem Mass Spectrometry (LC-MS/MS)

Concentrations of estradiol, estrone, testosterone, and androstenedione were measured by LC-MS/MS analysis in ASKA Pharma Medical Co., Ltd. (Kawasaki, Japan), as described previously [14, 15]. In the evaluation of estradiol concentration, we measured only 17β-estradiol, but not 17α-estradiol in this study. Briefly, tissue specimens were homogenized in 1 mL of distilled water, and steroid fraction was extracted with diethyl ether. In this study, we used an LC (Agilent 1100, Agilent Technologies, Waldbronn, Germany) coupled with an API 4000 triple-stage quadrupole

mass spectrometer (Applied Biosystems, Foster City, CA, USA) operated with electron spray ionization in the positive-ion mode, and the chromatographic separation was performed on Cadenza CD-C18 column (3×150 mm, 3.5 mm, Imtakt, Kyoto, Japan).

### Laser-Capture Microdissection (LCM)/Microarray Analysis

Gene expression profiles of MBC and FBC cells were examined by microarray analysis. Four MBC and four FBC tissues were subjected to the study. LCM was conducted using the MMI Cellcut (Molecular Machines and Industries, Flughofstrase, Glattbrugg, Switzerland) according to previous reports [14, 16]. Briefly, breast carcinoma specimens (one specimen for each case) were embedded in Tissue-Tek optimal cutting temperature compound (Sakura Finetechnical Co., Tokyo, Japan), and serial sections were made at a thickness of 10 μm. Sections were stained with toluidine blue according to manufacturer's recommendation, and subsequently, breast carcinoma cells in each specimen (approximately 5,000 cells) were dissected under light microscopy and laser transferred from the serial sections. The total RNA (approximately 200 ng) was subsequently extracted from these cell fractions isolated by LCM using the RNeasy® Micro Kit (QIAGEN, Mannheim, Germany). Gene expression profiles were examined by microarray analyses. Whole Human Genome Oligo Microarray (G4112F, ID: 012391, Agilent Technologies), containing 41,000 unique probes, was used in this study, and sample preparation and processing were performed according to the manufacturer's protocol.

In our present study, we focused upon the expression profiles of two gene lists which were previously reported as estrogen-induced genes in FBC cell line MCF-7 [4, 5]. One was Frasor's list which consisted of 50 genes [4], and the other was Creighton's list which consisted of 63 genes [5]. If a gene was represented multiple times on the platform, the probe with strongest positive correlation with ESR1 (ERα) was selected. In order to compare the expression profiles of these genes, unsupervised hierarchical clustering analysis was performed using the Cluster and TreeView programs (the software copyright Stanford University 1998–1999, http://rana.stanford.edu) to generate tree structures based on the degree of similarity, as well as matrices comparing the levels of expression of individual genes in each specimens. Expression of genes was statistically evaluated by Student's $t$ test, and $P<0.05$ was considered significant in this study.

### Immunohistochemistry

The characteristics of primary antibody of aromatase [13], STS [17], and 17βHSD1 [15] were described previously. Monoclonal antibodies for ERα (ER1D5), ERβ (14C8), PR (MAB429), and Ki-67 (MIB1) were purchased from Immunotech (Marseille, France), Gene Tex (San Antonio, TX, USA), Chemicon (Temecula, CA, USA), and DAKO (Carpinteria, CA, USA), respectively. Rabbit polyclonal antibody for HER2 (A0485) was obtained from DAKO. Rabbit polyclonal antibody for receptor interacting protein 140 (RIP140) and retinoic acid receptor α (RARα) were purchased from Santa Cruz Biotechnology (Santa Cruz, CA, USA).

A Histofine Kit (Nichirei Biosciences, Tokyo, Japan), which employs the streptavidin-biotin amplification method, was used in this study. Immunoreactivity of estrogen-producing enzymes was detected in the cytoplasm, and the cases that had more than 10 % of positive cells were considered positive [18, 19]. Immunoreactivity of ERα, ERβ, PR, Ki-67, RIP140, and RARα was detected in the nucleus. These immunoreactivities were evaluated in more than 1,000 carcinoma cells, and subsequently, the percentage of immunoreactivity, i.e., labeling index (LI), was determined [20]. HER2 immunoreactivity was evaluated according to a grading system proposed in HercepTest (DAKO), and the cases with strongly circumscribed membrane staining of HER2 in more than 10 % carcinoma cells (i.e., score 3+) were considered positive in this study.

## Results

### Tissue Concentration of Estrogens and Androgens in MBC

We first examined tissue concentration of sex steroids in non-neoplastic male breast, MBC, and FBC tissues by LC-MS/MS. Median with minimum–max value of the estradiol level was 37.0 (8.0–74.0)pg/g in non-neoplastic male breast, 523 (267–633)pg/g in MBC, and 190 (15.7–540) pg/g in FBC (Fig. 1a). Tissue concentration of estradiol was significantly ($P=0.03$ and 14-fold) higher in MBC than non-neoplastic male breast tissues. Moreover, intratumoral estradiol concentration was 2.8-fold higher in MBC than in FBC tissues, although $P$ value did not reach a significant level ($P=0.09$). On the other hand, tissue concentration of estrone was in 83.0 (56.0–359)pg/g in non-neoplastic male breast, 134 (67.0–280)pg/g in MBC, and 75.0 (13.0–555)pg/g in FBC, respectively, and the estrone level in MBC was not significantly different from that in non-neoplastic male breast or FBC ($P=0.72$ and $P=0.71$, respectively; Fig. 1b).

Tissue concentration of testosterone was high both in non-neoplastic male breast [1,519 (23.0–3,287)pg/g] and MBC [2,540 (1,454–3,483)pg/g], compared to that in FBC [133 (70.0–240)pg/g; $P=0.008$ in MBC vs. FBC], but no significant difference was detected between these two groups ($P=0.48$; Fig. 1c). Androstenedione has similar levels in these three groups [620 (53–7,525)pg/g in non-neoplastic male breast, 1,021 (291–1,805)pg/g in MBC, and 561 (160–5,785)pg/g in FBC] in this study (Fig. 1d).